*Inorg. Chem.* **2002**, *41*, 4405–4416


# Polynuclear Complexes of the Pendent-Arm Ligand 1,4,7-Tris(acetophenoneoxime)-1,4,7-triazacyclononane

**Vitaly Pavlishchuk, Frank Birkelbach, Thomas WeyhermÜller, Karl Wieghardt, and Phalguni Chaudhuri***

*Max-Planck-Institut für Strahlenchemie, Stiftstrasse 34-36, D-45470 Mülheim an der Ruhr, Germany*

Received December 27, 2001

The ligand 1,4,7-tris(acetophenoneoxime)-1,4,7-triazacyclononane ($H_3L$) has been synthesized and its coordination properties toward Cu(II), Ni(II), Co(II), and Mn(II) in the presence of air have been investigated. Copper(II) yields a mononuclear complex, $[Cu(H_2L)](ClO_4)$ (**1**), cobalt(II) and manganese(II) ions yield mixed-valence $Co^{III}_2Co^{II}$ (**2a**) and $Mn^{II}_2Mn^{III}$ (**4**) complexes, whereas nickel(II) produces a tetranuclear $[Ni_4(HL)_3]^{2+}$ (**3**) complex. The complexes have been structurally, magnetochemically, and spectroscopically characterized. Complex **3**, a planar trigonal-shaped tetranuclear Ni(II) species, exhibits irregular spin-ladder. Variable-temperature (2–290 K) magnetic susceptibility analysis of **3** demonstrates antiferromagnetic exchange interactions ($J = -13.4$ cm$^{-1}$) between the neighboring Ni(II) ions, which lead to the ground-state $S_t = 2.0$ owing to the topology of the spin-carriers in **3**. A bulk ferromaganetic interaction ($J = +2$ cm$^{-1}$) is prevailing between the neighboring high-spin Mn(II) and high-spin Mn(III) ions leading to a ground state of $S_t = 7.0$ for **4**. The large ground-state spin value of $S_t = 7.0$ has been confirmed by magnetization measurements at applied magnetic fields of 1, 4 and 7 T. A bridging monomethyl carbonato ligand formation occurs through an efficient $CO_2$ uptake from air in methanolic solutions containing a base in the case of complex **4**.

## Introduction

Since the introduction of dimethylglyoxime[1] as a ligand for a transition metal ion, viz. Ni(II), at the beginning of 20th century, oximes have played a notable role in the development of transition metal coordination chemistry, because of their rich chemistry and variety of bonding modes: only N-, only O-, or both N- and O-binding sites.[2] A remarkable feature of the oxime ligands is their propensity to form polynuclear complexes,[3−17] both homo- and hetero-nuclear, in which oxime function (═N−O) acts as a bridging unit to yield magnetically interesting compounds which can be potentially useful for the development of new materials in the field of molecular magnetism.[18,19] Additionally, deprotonated oxime groups have been demonstrated to

* Author to whom correspondence should be addressed. E-mail: chaudh@mpi-muelheim.mpg.de.

(1) (a) Chugaev, L. A. *Chem. Ber.* **1905**, *38*, 2520. (b) Chugaev, L. A. *J. Chem. Soc., London* **1914**, *105*, 2187.
(2) (a) Mehrotra, R. C. In *Comprehensive Coordination Chemistry*; Wilkinson, G., Gillard, R. D., McCleverty, J. A., Eds.; Pergamon Press: Oxford, UK, 1987; Vol. 2, p 269. (b) Chakravorty, A. *Coord. Chem. Rev.* **1974**, *13*, 1. (c) Schrauzer, G. N. *Angew. Chem.* **1976**, *88*, 465. (d) Samus, N. M.; Ablov, A. V. *Coord. Chem. Rev.* **1979**, *28*, 177. (e) Kukushkin, V. Y.; Pombeiro, A. J. L. *Coord. Chem. Rev.* **1999**, *181*, 147.
(3) (a) Beckett, R.; Colton, R.; Hoskins, B. F.; Martin, R. L.; Vince, D. G. *Aust. J. Chem.* **1969**, *22*, 2527. (b) Beckett, R.; Hoskins, B. F. *J. Chem. Soc., Dalton Trans.* **1972**, 291.
(4) Bertrand, J. A.; Smith, J. H.; Garyeller, P. *Inorg. Chem.* **1974**, *13*, 1649.
(5) (a) Mohanty, J. G.; Baral, S.; Singh, R. P.; Chakravorty, A. *Inorg. Nucl. Chem. Lett.* **1974**, *10*, 655. (b) Datta, D.; Chakravorty, A. *Inorg. Chem.* **1983**, *22*, 1611. (c) Pal, S.; Mukherjee, R.; Tomas, M.; Falvello, L. R.; Chakravorty, A. *Inorg. Chem.* **1986**, *25*, 200. (d) Basu, P.; Pal, S.; Chakravorty, A. *Inorg. Chem.* **1988**, 27, 1850. (e) Chatlopadhyay, S.; Basu, P.; Pal, S.; Chakravorty, A. *J. Chem. Soc., Dalton Trans.* **1990**, 3829. (f) Ganguly, S.; Karmakar, S.; Pal, C. K.; Chakravorty, A. *Inorg. Chem.* **1999**, *38*, 5984 and references therein.
(6) (a) Okawa, H.; Koikawa, M.; Kida, S.; Luneau, D.; Oshio, H. *J. Chem. Soc., Dalton Trans.* **1990**, 469. (b) Luneau, D.; Oshio, H.; Okawa, H.; Koikawa, M.; Kida, S. *Bull. Chem. Soc. Jpn.* **1990**, *63*, 2212. (c) Luneau, D.; Oshio, H.; Okawa, H.; Kida, S. *J. Chem. Soc., Dalton Trans.* **1990**, 2282. (d) Zhong, Z. J.; Okawa, H.; Matsumoto, M.; Sakiyama, H.; Kida, S. *J. Chem. Soc., Dalton Trans.* **1991**, 497. (e) Fukita, N.; Ohba, M.; Shig, T.; Okawa, H.; Ajiro, Y. *J. Chem. Soc., Dalton Trans.* **2001**, 64.
(7) Agnus, Y.; Louis, R.; Metz, B.; Boudin, C.; Gisselbrecht, J. P.; Gross, M. *Inorg. Chem.* **1991**, *30*, 3155.
(8) Colacio, E.; Domiguez-Vera, J. M.; Escuer, A.; Kivekas, R.; Romerosa, A. *Inorg. Chem.* **1994**, *33*, 3911.
(9) Rybak-Akimova, E. V.; Busch, D. H.; Kahol, P. K.; Pinto, N.; Alcock, N. W.; Clase, H. J. *Inorg. Chem.* **1997**, *36*, 510.

10.1021/ic011322m CCC: $22.00 
Published on Web 07/31/2002

stabilize high oxidation states at the metal sites, viz. Ni(III), Ni(IV), and Cu(III).[20−22]

In another field of research, an enormous growth of pendent-arm derivatives[23−27] of azamacrocyclic ligands has been witnessed during the past two decades, as they provide a useful control over the ligand environment around transition metal ions. Thus, these macrocyclic polyfunctional ligands have found applications in different areas ranging from analytical chemistry to biochemistry and medicine.[28] 1,4,7-Triazacyclononane (TACN)[27,29] is now well-established as a transition metal coordinating ligand and used for the synthesis of high- and low-valent organometallics, as well as for the preparation of models of metallobiosites, due to their ability to form stable complexes with metal ions. As part of ongoing efforts to produce novel polynuclear metal complexes with oximes as ligands[15] and our continuous interest in utilizing TACN-based ligands,[30] we have synthesized a new member of the *N*-functionalized pendent-armed TACN series. There are of course many examples of triazacyclononane derivatives with pendent arms such as $CH_2CO_2H$,[31,32] $CH_2CH_2OH$,[33] $CH_2C_6H_4OH$,[34] $CH_2C_6H_4SH$,[35] $CH_2C_6H_4NH_2$,[36] $CH_2CH_2NH_2$,[37] $CH_2C_5H_4N$,[38] $CH_2PO_3H_2$,[37] $CH_2CONHCH(CH_2Ph)CO_2Me$,[38] bipyridylmethyl,[39] imidazolylmethyl,[40] pyrazolylmethyl,[41] 2,2′:6,2″-terpyridylmethyl,[42] 2-aminophenyl,[43] etc. We felt it would be interesting to examine the effect of attaching oxime donor groups to the macrocyclic secondary amine positions. Not only would this impart upon the ligand additional denticity, but it would also be expected to increase the strength of the ligand field through incorporation of azomethine nitrogens. To this end we have devised a simple synthesis of the pendent-arm ligand 1,4,7-tris(acetophenoneoxime)-1,4,7-triazacyclononane ($H_3L$) and have begun to explore its transition metal coordination chemistry. Here we describe a new ligand system that incorporates two particularly efficient stabilizing fragments: a combination of azamacrocycle and strong ligand-field oxime within the same ligand framework. It was anticipated that the mentioned combination may stabilize some unusual oxidation states and $H_3L$ would be able to form complexes with different nuclearity. This expectation was confirmed as the ligand afforded polynuclear nickel, cobalt, and manganese chelates, which are authenticated by structure


(10) (a) Ruiz, R.; Lloret, F.; Julve, M.; Faus, J.; Munoz, M. C.; Solans, X. *Inorg. Chim. Acta* **1993**, *213*, 261. (b) Lloret, F.; Ruiz, R.; Julve, M.; Faus, J.; Journaux, Y.; Castro, I.; Verdagner, M. *Chem. Mater.* **1992**, *4*, 1150. (c) Cervera, B.; Ruiz, R.; Lloret, F.; Julve, M.; Cano, J.; Faus, J.; Bois, C.; Mrozinski, J. *J. Chem. Soc., Dalton Trans* **1997**, 395. (d) Ruiz, R.; Julve, M.; Faus, J.; Lloret, F.; Munoz, C. M.; Journaux, Y.; Bois, C. *Inorg. Chem.* **1997**, *36*, 3434. (e) Cervera, B.; Ruiz, R.; Lloret, F.; Julve, M.; Faus, J.; Munoz, C. M.; Journaux, Y. *Inorg. Chim. Acta* **1999**, *288*, 57.

(11) Black, D.; Blake, A. J.; Dancey, K. P.; Harrison, A.; McPartlin, M.; Parsons, S.; Tasker, P. A.; Whittaker, G.; Schröder, M. *J. Chem. Soc., Dalton Trans.* **1998**, 395.

(12) Thorpe, J. M.; Beddoes, R. L.; Collison, D.; Garner, C. D.; Helliwell, M.; Holmes, J. M.; Tasker, P. A. *Angew. Chem., Int. Ed. Engl.* **1999**, *38*, 1119.

(13) (a) Chaudhuri, P.; Winter, M.; Fleischhauer, P.; Haase, W.; Flörke, U.; Haupt, H.-J. *J. Chem. Soc., Chem. Commun.* **1990**, 1728. (b) Chaudhuri, P.; Winter, M.; Della Védova, B. P. C.; Fleischhauer, P.; Haase, W.; Flörke, U.; Haupt, H.-J. *Inorg. Chem.* **1991**, *30*, 4777. (c) Burdinski, D.; Bill, E.; Birkelbach, F.; Wieghardt, K.; Chaudhuri, P. *Inorg. Chem.* **2001**, *40*, 1160 and references therein.

(14) (a) Birkelbach, F.; Winter, M.; Flörke, U.; Haupt, H.-J.; Butzlaff, C.; Lengen, M.; Bill, E.; Trautwein, A. X.; Wieghardt, K.; Chaudhuri, P. *Inorg. Chem.* **1994**, *33*, 3990. (b) Chaudhuri, P.; Winter, M.; Flörke, U.; Haupt, H.-J. *Inorg. Chim. Acta* **1995**, *232*, 125. (c) Verani, C. N.; Bothe, E.; Burdinski, D.; Weyhermüller, T.; Flörke, U.; Chaudhuri, P. *Eur. J. Inorg. Chem.* **2001**, 2161 and references therein.

(15) (a) Verani, C. N.; Rentschler, E.; Weyhermüller, T.; Bill, E.; Chaudhuri, P. *J. Chem. Soc., Dalton Trans.* **2000**, 4263 and references therein. (b) Chaudhuri, P. *Proc. Indian Acad. Sci. (Chem. Sci.)* **1999**, *111*, 397.

(16) (a) Chaudhuri, P.; Birkelbach, F.; Winter, M.; Staemmler, V.; Fleichhauer, P.; Haase, W.; Flörke, W.; Haupt, H.-J. *J. Chem. Soc., Dalton Trans.* **1994**, 2313. (b) Krebs, C.; Winter, M.; Weyhermüller, T.; Bill, E.; Wieghardt, K.; Chaudhuri, P. *J. Chem. Soc., Chem. Commun.* **1995**, 1913.

(17) Chaudhuri, P.; Hess, M.; Rentschler, E.; Weyhermüller, T.; Flörke, U. *New J. Chem.* **1998**, 553.

(18) (a) Kahn, O. *Molecular Magnetism*; VCH Verlagsgesellschaft mbH: Weinheim, Germany, 1993. (b) Kahn, O. In *Advances in Inorganic Chemistry*; Sykes, A. G., Ed.; Academic Press: New York, 19XX; Vol. 43, p 179.

(19) *Magnetic Molecular Materials*; Gatteschi, D., Kahn, O., Miller, J. S., Palacio, F., Eds.; NATO ASI Ser. 198; Kluwer: Dordrecht, The Netherlands, 1991.

(20) (a) Sulfab, Y.; Al-Shatti, N. I. *Inorg. Chim. Acta* **1984**, *87*, L23. (b) Sulfab, Y.; Hussein, M. A.; Al-Shatti, N. I. *Inorg. Chim. Acta* **1982**, *67*, L33.

(21) Hanss, J.; Beckmann, A.; Krüger, H.-J. *Eur. J. Inorg. Chem.* **1999**, 163.

(22) (a) Nag, K.; Chakravorty, A. *Coord. Chem. Rev.* **1980**, 33, 8. (b) Chakravorty, A. *Isr. J. Chem.* **1985**, *25*, 99.

(23) Kaden, T. A. *Top. Curr. Chem.* **1984**, *121*, 154.

(24) Bernhardt, P. V.; Lawrence, G. A. *Coord. Chem. Rev.* **1990**, *104*, 297.

(25) Hancock, R. D.; Maumela, H.; de Sousa, A. S. *Coord. Chem. Rev.* **1996**, *148*, 315.

(26) Wainwright, K. P. *Coord. Chem. Rev.* **1997**, *166*, 35.

(27) Chaudhuri, P.; Wieghardt, K. *Prog. Inorg. Chem.* **1987**, *35*, 329.

(28) Kaden, T. A. *Chimica* **2000**, *54*, 574.

(29) (a) Tolman, W. B. *Acc. Chem. Res.* **1997**, *30*, 227. (b) Chan, M. C. W.; Lee, F. W.; Cheung, K. K.; Che, C. M. *J. Chem. Soc., Dalton Trans.* **1999**, 3197. (c) Giesbrecht, G. R.; Shafir, A.; Arnold, J. *Chem. Commun.* **2000**, 2135. (d) Fletcher, J. S.; Male, N. A. H.; Wilson, P. J.; Rees, L. H.; Mountford, P.; Schröder, M. *J. Chem. Soc., Dalton Trans.* **2000**, 4130. (e) Robson, D. A.; Rees, L. H.; Mountford, P.; Schröder, M. *Chem. Commun.* **2000**, 1269. (f) Qian, B.; Henling, L. M.; Peters, J. C. *Organometallics* **2000**, *19*, 2805. (g) Bambirra, S.; van Leusen, D. U.; Meetsma, A.; Hessen, B.; Teupen, J. H. *Chem. Commun.* **2001**, 637. (h) Robson, D. A.; Bylikin, S. Y.; Cantuel, M.; Male, N. A. H.; Rees, L. H.; Mountford, P.; Schröder, M. *J. Chem. Soc., Dalton Trans.* **2001**, 157. (i) Bylikin, S. Y.; Robson, D. A.; Male, N. A. H.; Rees, L. H.; Mountford, P.; Schröder, M. *J. Chem. Soc., Dalton Trans.* **2001**, 170.

(30) Weyhermüller, T.; Wieghardt, K.; Chaudhuri, P. *J. Chem. Soc., Dalton Trans.* **1998**, 3805.

(31) Takahasi, M.; Takamoto, S. *Bull. Chem. Soc. Jpn.* **1977**, *50*, 3413.

(32) Wieghardt, K.; Bossek, U.; Chaudhuri, P.; Herrmann, W.; Menke, B. C.; Weiss, J. *Inorg. Chem.* **1982**, *21*, 4308.

(33) Sayer, B. A.; Michael, J. P.; Hancock, R. D. *Inorg. Chim. Acta* **1983**, *77*, L63.

(34) Moore, D. A.; Fanwick, P. E.; Welch, M. J. *Inorg. Chem.* **1989**, *28*, 1504.

(35) Beissel, T.; Bürger, K. S.; Voigt, G.; Wieghardt, K.; Butzlaff, C.; Trautwein, A. X. *Inorg. Chem.* **1993**, *32*, 124.

(36) Schlager, O.; Wieghardt, K.; Grondey, H.; Rufinska, A.; Nuber, B. *Inorg. Chem.* **1995**, *34*, 6440.

(37) Gahan, L. R.; Lawrence, G. A.; Sargeson, A. M. *Aust. J. Chem.* **1982**, *35*, 1119.

(38) (a) Christiansen, L.; Hendrickson, D. N.; Toflund, H.; Wilson, S. R.; Xie, C. L. *Inorg. Chem.* **1986**, *25*, 2813. (b) Wieghardt, K.; Schöffmann, E.; Nuber, B.; Weiss, J. *Inorg. Chem.* **1986**, *25*, 4877.

(39) Ziessel, R.; Lehn, J.-M. *Helv. Chim. Acta* **1990**, *73*, 1149.

(40) Di Vaira, M.; Manni, F.; Stoppioni, P. *J. Chem. Soc., Chem. Commun.* **1989**, 126.

(41) Di Vaira, M.; Cosimelli, B.; Manni, F.; Stoppioni, P. *J. Chem. Soc., Dalton Trans.* **1991**, 331.

(42) Alcock, N. W.; Clarke, A. J.; Errington, W.; Jasceanu, A. M.; Moore, P.; Rawle, S. C.; Sheldon, P.; Smith, S. M.; Turonek, M. L. *Supramol. Chem.* **1996**, *6*, 281.

(43) Fallis, I. A.; Farley, R. D.; Abdul Malik, K. M.; Murphy, D. M.; Smith, H. J. *J. Chem. Soc., Dalton Trans.* **2000**, 3632.

determinations, the results of which are described herein. In particular, the versatility of $H_3L$ will be shown. Further, it is hoped that this investigation might be used as a predictive tool to elucidate the coordination chemistry of such oxime-containing azamacrocycles with other, as yet unexplored, Lewis acids. It is relevant to mention here that we have also synthesized tris($CH_2C(CH_3)$═N−OH)[44] and tris($CH_2C(NH_2)$═N−OH)[44] derivatives of TACN, which will be published in a forthcoming paper.

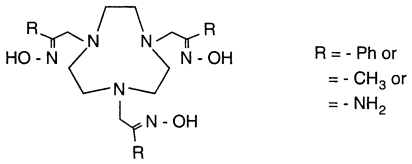


## Results and Discussion

The ligand 1,4,7-tris(acetophenoneoxime)-1,4,7-triazacyclononane was prepared by the reaction of 3 equiv of *ω*-chloroacetophenoneoxime with the free amine 1,4,7-triazacyclononane in the presence of sodium bicarbonate. The ligand as colorless trihydrochloride was conveniently isolated in good yield and its purity established by IR, NMR, and mass spectrometry. The transition metal complexes, prepared in methanol from the respective metal salts and free base form of the ligand $H_3L$, were isolated as perchlorate salts.

Although the ligand has three potentially dissociable protons present as OH groups in the oxime part of the ligand, deprotonation upon reaction with different metal ions in the equivalent conditions is dependent on the nature of the metal ions, as is shown by differently protonated ligands present in isolated complexes. For example, the diprotonated monoanion $H_2L^-$ is coordinated to the copper(II) center to yield a mononuclear complex **1**. On the other hand, $HL^{2-}$ is present both in the tetranuclear Ni(II) **3** and in trinuclear mixed-valence $Mn^{II}Mn^{III}Mn^{II}$ complex, **4**, whereas the ligand is fully deprotonated $L^{3-}$ in the cobalt complexes **2** and **2a**.

The reaction of $Mn(ClO_4)_2 \cdot 6H_2O$ in methanol with the ligand $H_3L$ in the presence of air yields deep brown crystals of $[(LH)_2Mn^{II}_2(\mu\text{-}OOC \cdot OCH_3)(CH_3OH)Mn^{III}](ClO_4)_2 \cdot 2CH_3OH \cdot 3H_2O$, **4**, in which the ligand is monoprotonated with one of the oxime groups protonated and noncoordinated. Interestingly, a bridging monomethyl carbonato ligand formation occurs through the $CO_2$ uptake from air by the methanolic solutions containing $NEt_3$ as a base, presumably according to the following reaction:

$$CH_3OH + CO_2 + NEt_3 \underset{Mn^{2+}/H_3L}{\rightleftharpoons} CH_3O\,CO_2^- + HNEt_3^+$$

Carbon dioxide is taken up from the air spontaneously and the monomethyl carbonato complex was isolated as a single product. Monomethyl carbonato complexes[45] synthesized through an efficient $CO_2$ uptake have also been reported for other metal centers such as Co, Ni, and Zn.

Addition of base was necessary to make the preparation of the monomethyl carbonato complex of manganese efficient. In contrast, no monomethyl carbonato complex for Ni(II) was observed even in the presence of added base. These results together with the reported monomethyl carbonato complexes obtained by facile $CO_2$ uptake from the air indicate that the chemical reactivity is based on the Lewis acidity of the complexes and not restricted to a specific metal $d^n$-electron configuration.

The IR spectra of all the complexes derived from $H_3L$ exhibit characteristic bands due to the ligand [$\nu$(OH), $\nu$(C═N), $\nu$(NO) at about ≈3430, ≈1620, and ≈1120 $cm^{-1}$, respectively], and noncoordinated perchlorate anions [≈1100 and ≈625 $cm^{-1}$]. In the case of **4**, the trinuclear manganese complex, a strong sharp band observed at 1637 $cm^{-1}$ can be attributed to the presence of the monomethyl carbonato group, while for **1**, **2**, and **3**, this band is absent and a medium strong band is observed at ≈1620 $cm^{-1}$, a region where the $\nu$(CN) vibrations appear.

The two CO stretching vibrational bands $\nu_1$ and $\nu_2$ in the infrared spectrum of **4** reflect the bridging coordination mode of the monomethyl carbonato ligand. That is, the strong $\nu_1$ band at 1637 $cm^{-1}$ and a weaker $\nu_2$ band at 1335 $cm^{-1}$ result in the difference ($\Delta\nu = \nu_1 - \nu_2$) of 302 $cm^{-1}$, which is smaller than that in the free ion $CH_3OCO_2^-$. The free $CH_3OCO_2^-$ ion shows $\nu_1$ at 1640 $cm^{-1}$ and $\nu_2$ at 1310 $cm^{-1}$, and thus $\Delta\nu$ amounts to 330 $cm^{-1}$.[45] Thus IR data strongly suggest that $CH_3OCO_2^-$ is involved in bridging or multidentate coordination, which is in conformity with the X-ray structural determination of **4**.

**Electrospray-Ionization Mass Spectrometry (ESI-MS).** Mass spectrometry in the ESI-positive mode in $CH_3OH$ and $CH_3CN$ has proved to be a very useful tool to demonstrate the nuclearity of **1**, **3**, and **4** and also provided identification of the metal centers. There was practically no indication in the spectra for oxime−ligand fragmentation, but cleavage of the polynuclear complexes to smaller entities was indicated. A single molecular ion peak centered around *m*/*z* 590 (100%) for **1** confirms the formulation $[CuLH_2]^+$ with the diprotonated ligand. Complex **2a** exhibits only a few peaks, of which two intense peaks centered around *m*/*z* 585 (100%) and 1169 (20%) correspond to the mononuclear $[Co(LH)]^+$ and dinuclear $[Co_2(LH)_2]^+$ ions, respectively. There was no peak for the trinuclear entity (**2**, **2a**); the X-ray structure of **2** is described later.

The base peak for **3** is observed at *m*/*z* 585.2 (100%) corresponding to the monocharged $[Ni(H_2L)]^+$ species. Interestingly, although the dimeric form $[Ni_2(H_3L_2)]^+$ is observed at *m*/*z* 1169.8 with an abundance of 60%, no molecule ion peak, i.e., the tetrameric Ni(II) form, was observed. Two weak signals (∼5%) corresponding to the doubly charged species of the tetranuclear form, i.e., $[(LH)_3Ni_4]^{2+}$ at *m*/*z* 907.2 and 1227.7 assigned to monocharged species $[Ni_3(LH)_2]^+$, also appeared in the ESI-MS spectrum for **3**.

(44) (a) Birkelbach, F. Dissertation, Bochum, 1995. (b) Chaudhuri, P.; Winter, M.; Flörke, U. Unpublished work.

(45) (a) Kato, M.; Ito, T. *Inorg. Chem.* **1985**, *24*, 504. (b) Kato, M.; Ito, T. *Inorg. Chem.* **1985**, *24*, 509. (c) Kato, M.; Ito, T. *Bull. Chem. Soc. Jpn.* **1986**, *59*, 285. (d) Hosokawa, Y.; Yamane, H.; Nakao, Y.; Matsumoto, K.; Takamizawa, S.; Mori, W.; Suzuki, S. *Chem. Lett.* **1997**, 891.

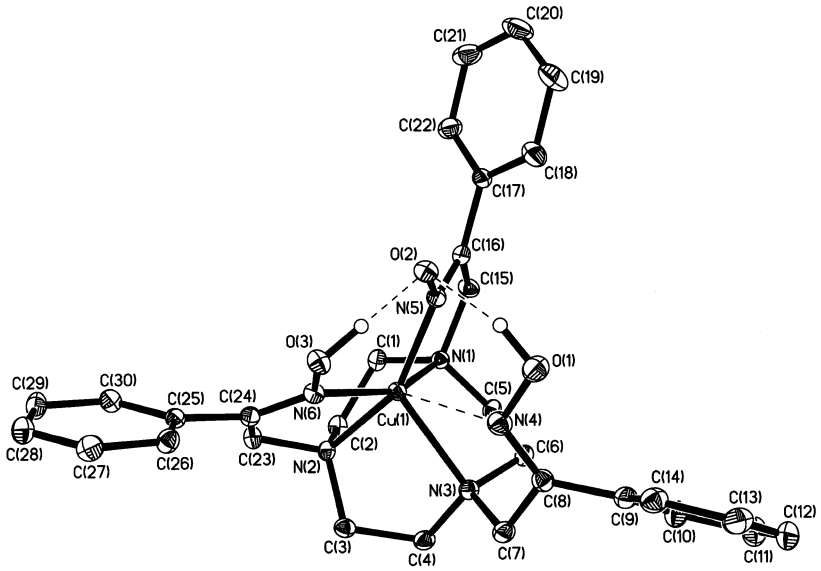


**Figure 1.** ORTEP drawing of the monocation $[Cu(LH_2)]^+$ in **1**.

**Table 1.** Selected Bond Lengths (Å) and Angles (deg) for $[Cu(LH_2)]ClO_4 \cdot CH_3OH$ (**1**)

| | | | |
|---|---|---|---|
| Cu(1)−N(5) | 1.943(2) | N(5)−Cu(1)−N(6) | 93.08(7) |
| Cu(1)−N(6) | 1.954(2) | N(5)−Cu(1)−N(1) | 84.19(7) |
| Cu(1)−N(1) | 2.038(2) | N(6)−Cu(1)−N(1) | 151.79(7) |
| Cu(1)−N(2) | 2.047(2) | N(5)−Cu(1)−N(2) | 152.81(7) |
| Cu(1)−N(3) | 2.260(2) | N(6)−Cu(1)−N(2) | 81.85(7) |
| | | N(1)−Cu(1)−N(2) | 87.86(7) |
| O(1)−N(4) | 1.394(2) | N(5)−Cu(1)−N(3) | 122.06(7) |
| O(2)−N(5) | 1.364(2) | N(6)−Cu(1)−N(3) | 120.89(7) |
| O(3)−N(6) | 1.369(2) | N(1)−Cu(1)−N(3) | 83.31(7) |
| | | N(2)−Cu(1)−N(3) | 82.52(7) |

The spectrum of **4** exhibits the base peak at *m*/*z* 608.3, which corresponds to the doubly charged species $[(LH)_2Mn_3]^{2+}$. There was no indication of the molecule ion peak, presumably due to easy dissociation of monomethyl carbonate and methanol groups from **4**. A small signal at *m*/*z* 1315.5 is assignable to the monocharged species $[(LH)_2Mn_3(ClO_4)]^+$.

**Molecular Structure of $[LH_2Cu^{II}]ClO_4 \cdot CH_3OH$ (1).** The complex molecule consists of a monocationic mononuclear unit, a perchlorate anion, and a methanol molecule. The cation together with the atomic labeling scheme used is shown in Figure 1. Selected bond lengths and angles are listed in Table 1. The cation geometry is approximately trigonal bipyramidal, where N(1) and N(3) of the cyclic amine and N(6) of a pendent oxime group occupy the three sites of the equatorial plane and the two axial sites of the polyhedron are occupied by N(2) of the cyclic amine and N(5) of an oxime group. The three equatorial N−Cu−N angles are 120.89°, 83.3°, and 151.8°, different from those required for an idealized trigonal bipyramid, presumably as a consequence of the restricted ligand bite. The Cu−N distances of 2.048(av) Å are considered as normal covalent bonds. The equatorial Cu−N(3) bond is significantly longer, 2.260(2) Å, as has been observed earlier for the macrocyclic amine.[27] The Cu(1)···N(4) distance of 2.835(2) Å is long to be considered as a covalent bond. The O(3)···O(2) and O(1)···O(2) distances of 2.481(3) and 2.710(3) Å, respectively, are clearly indicative of strong hydrogen bond interactions, suggesting nonligated O(3) and O(1) are protonated. Indeed, a difference Fourier in the later refinement stages did reveal peaks assignable to these protons, appearing approximately equidistant from the two oxygen atoms, and they were included in these positions in the final refinement cycle.

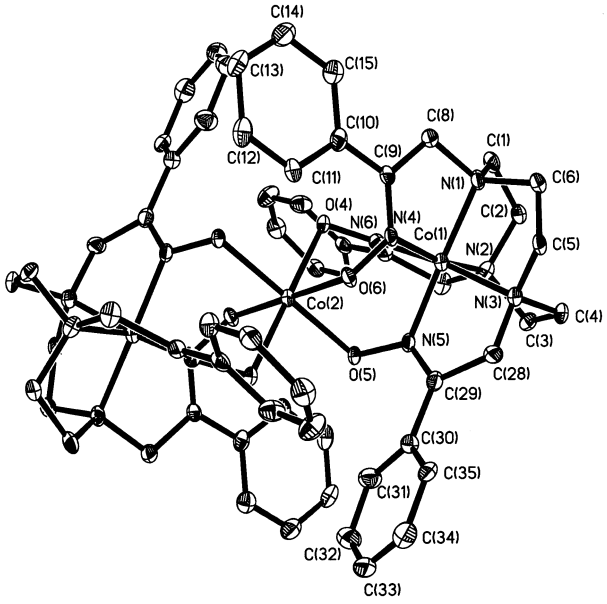


**Figure 2.** Structure of the cation $[L_2Co^{III}_2Co^{II}]^{2+}$ in the crystal of **2**.

**X-ray Structure of $[L_2Co^{III}_2Co^{II}](ClO_4)_2 \cdot H_2O \cdot Et_2O \cdot Me_2CO$ (2).** The molecular geometry and the atom-labeling scheme of the cation in **2** is shown in Figure 2. The structure of the complex consists of a discrete dicationic trinuclear centrosymmetric unit having a crystallographic 2-fold symmetry, two noncoordinatively bound perchlorate anions, and solvent molecules. Selected bond lengths and angles are presented in Table 2. The X-ray structure confirms that a linear trinuclear complex, Co(1)−Co(2)−Co(1a) = 180°, is formed in such a way that two $Co^{III}L$ fragments coordinate the centrally placed Co(II) ion. The central Co(2) is octahedrally bonded by six oximato oxygen atoms pendent from the two CoL fragments. The octahedron is as expected not exactly regular, with Co(2)−O bond distances varying

**Table 2.** Important Interatomic Distances (Å) and Angles (deg) for the Cation $[L_2Co^{III}_2Co^{II}]^{2+}$ in **2**

| | | | |
|---|---|---|---|
| Co(1)−N(5) | 1.885(4) | | |
| Co(1)−N(4) | 1.897(4) | | |
| Co(1)−N(6) | 1.898(4) | N(4)−C(19) | 1.283(6) |
| Co(1)−N(1) | 1.943(4) | N(4)−O(4) | 1.317(4) |
| Co(1)−N(2) | 1.945(4) | N(5)−C(29) | 1.299(6) |
| Co(1)−N(3) | 1.961(4) | N(5)−O(5) | 1.325(4) |
| Co(2)−O(5) | 2.082(3) | N(6)−C(9) | 1.292(6) |
| Co(2)−O(6) | 2.118(3) | N(6)−O(6) | 1.336(4) |
| Co(2)−O(4) | 2.129(3) | | |
| N(5)−Co(1)−N(4) | 90.3(2) | | |
| N(5)−Co(1)−N(6) | 89.5(2) | C(19)−N(4)−O(4) | 121.4(4) |
| N(4)−Co(1)−N(6) | 90.0(2) | C(29)−N(5)−O(5) | 121.0(4) |
| N(5)−Co(1)−N(1) | 169.6(2) | C(9)−N(6)−O(6) | 120.8(4) |
| N(4)−Co(1)−N(1) | 97.6(2) | | |
| N(6)−Co(1)−N(1) | 83.6(2) | | |
| N(5)−Co(1)−N(2) | 99.8(2) | | |
| N(4)−Co(1)−N(2) | 83.7(2) | Co(1)···Co(2) | 3.402(2) |
| N(6)−Co(1)−N(2) | 168.8(2) | Co(1)···Co(1a) | 6.805(4) |
| N(1)−Co(1)−N(2) | 88.0(2) | | |
| N(5)−Co(1)−N(3) | 84.3(2) | | |
| N(4)−Co(1)−N(3) | 169.1(2) | | |
| N(6)−Co(1)−N(3) | 99.4(2) | | |
| N(1)−Co(1)−N(3) | 89.0(2) | | |
| N(2)−Co(1)−N(3) | 87.9(2) | | |
| O(5)#1−Co(2)−O(5) | 179.998(1) | | |
| O(5)#1−Co(2)−O(6)#1 | 89.82(12) | | |
| O(5)−Co(2)−O(6)#1 | 90.18(12) | | |
| O(5)#1−Co(2)−O(6) | 90.18(12) | | |
| O(5)−Co(2)−O(6) | 89.82(12) | | |
| O(6)#1−Co(2)−O(6) | 180.0 | | |
| O(5)#1−Co(2)−O(4)#1 | 91.14(12) | | |
| O(5)−Co(2)−O(4)#1 | 88.86(12) | | |
| O(6)#1−Co(2)−O(4)#1 | 91.96(11) | | |
| O(6)−Co(2)−O(4)#1 | 88.04(11) | | |
| O(5)#1−Co(2)−O(4) | 88.86(12) | | |
| O(5)−Co(2)−O(4) | 91.14(12) | | |
| O(6)#1−Co(2)−O(4) | 88.04(11) | | |
| O(6)−Co(2)−O(4) | 91.96(11) | | |
| O(4)#1−Co(2)−O(4) | 179.997(1) | | |

between 2.082(3) and 2.129(3) Å, and the cis O−Co(2)−O bond angles are within 2° of the octahedral value of 90°. In salt hydrates having the $Co(OH_2)_6^{2+}$ ion the $CoO_6$ sphere is invariably a distorted octahedron and the average Co−O bond length, like that in the cation of **2**, lies very close to 2.08(5) Å.[48] The same applies to $[Co(PyO)_6]^{2+}$ (PyO = pyridine-*N*-oxide) with the average Co−O bond distance of 2.086(4) Å.[49] The Co(2)−O(5) distance of 2.082(3) Å in **2** is significantly shorter than the other two Co(2)−O(6) and Co(2)−O(4) bond lengths of 2.118(3) and 2.129(3) Å, respectively, as is expected for an axially compressed Jahn−Teller ion. We recall that the high-spin Co(II) ($t_{2g}^5e_g^2$) complexes are susceptible to Jahn−Teller distortions although the structural effect would be expected to be considerably less pronounced, since the degeneracy occurs in the $t_{2g}$ d-orbital set rather than in the $e_g$ set. Thus, the structural data confirm the high-spin $d^7$ electronic configuration of Co(2) in **2**, which is also corroborated with its paramagnetism. The nearest neighbor Co(1)···Co(2) distance within the trinuclear cation is 3.402(2) Å.

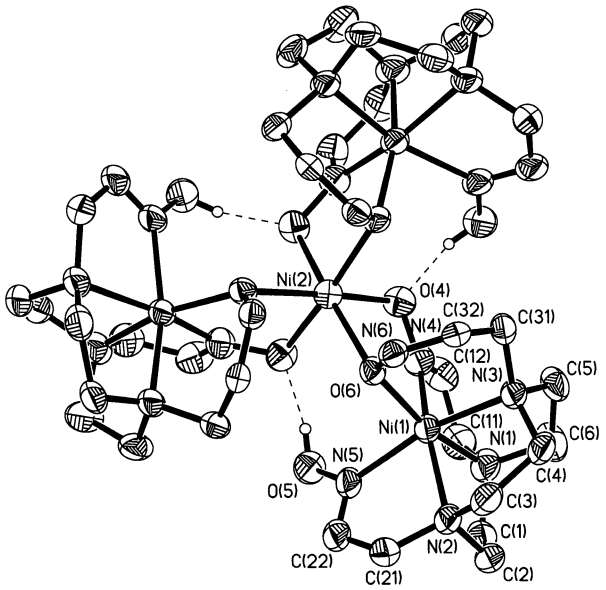


**Figure 3.** Molecular structure of the complex cation $[Ni_4(LH)_3]^{2+}$ in **3** showing the atom-numbering scheme. The phenyl groups attached to C(12), C(22), and C(32) are omitted for clarity.

The coordination geometry of the terminal cobalt atom, Co(1), is distorted octahedral with nitrogen atoms N(1), N(2), and N(3) from the facially coordinated macrocyclic amine unit and three nitrogen atoms N(4), N(5), and N(6) from the pendent oxime, resulting in the $CoN_6$ chromophore. The Co(1)−N (1, 2, or 3) (average 1.950(8) Å) and Co(1)−N (4, 5, or 6) (average 1.893(8) Å) distances are in accord with the low-spin description of the Co(III) centers with comparable donor ligands. The largest deviation from the ideal 90° interbond angles occurs for N(6)−Co(1)−N(3) with 99.4(2)°. An *intramolecular* Co(1)···Co(1a) separation of 6.804(4) Å has been found.

The N−O (average 1.326(10) Å) and C═N (average 1.291(8) Å) bond lengths and C−N−O bond angle (average 121.1(3)°) of the bridging oximato ligands are comparable to those found in the literature.[2]

**Molecular Structure of $[Ni_4(LH)_3](ClO_4)_2\cdot 3H_2O$ (3).** The structure consists of discrete tetranuclear dications $[Ni_4(LH)_3]^{2+}$, perchlorate anions, and water molecules. A view of the entire complex cation is given in Figure 3. For the sake of clarity the phenyl groups attached to C(12), C(22), and C(32) are omitted. Relevant bond distances and angles are listed in Table 3.

The complex cation has crystallographically imposed $C_3$ symmetry. The Ni(2) atom lies on the 3-fold axis and is surrounded by six oximic oxygens, O(4), O(6), and their equivalents, which are bonded to azomethine nitrogens N(4) and N(6), to serve as pairwise bridges to three crystallo-

(46) Wieghardt, K.; Schmidt, W.; Nuber, B.; Weiss, J. *Chem. Ber.* **1979**, *112*, 2220.
(47) Atkins, T. J.; Richman, J. E.; Oettle, W. F. *Org. Synth.* **1978**, *58*, 86.
(48) (a) Lynton, H.; Siew, P. Y. *Can. J. Chem.* **1997**, *51*, 2227. (b) Nassimbeni, L. R.; Percy, G. C.; Rodgers, A. L. *Acta Crystallogr.* **1976**, *B32*, 1252. (c) Adiwidjaja, G.; Rossmanith, E.; Küppers, H. *Acta Crystallogr.* **1978**, *B34*, 3079. (d) Knuuthila, P. *Inorg. Chim. Acta* **1981**, *52*, 141. (e) Riley, P. E.; Pecoraro, V. L.; Carrano, C. J.; Raymond, K. N. *Inorg. Chem.* **1983**, *22*, 3096. (f) Ward, D. L.; Luehrs, D. C. *Acta Crystallogr.* **1983**, *C39*, 1370. (g) Ganesh, V.; Seshasayee, M.; Aravamudan, G.; Heijdenrijk, D.; Schenk, H. *Acta Crystallogr.* **1990**, *C46*, 949. (h) Kosnic, E. J.; McClymont, E. L.; Hodder, R. A.; Squattrito, P. J. *Inorg. Chim. Acta* **1992**, *201*, 143. (i) Steed, J. W.; McCool, B. J.; Junk, P. C. *J. Chem. Soc., Dalton Trans.* **1998**, 3417.
(49) (a) Bergendahl, T. J.; Wood, J. S. *Inorg. Chem.* **1975**, *14*, 338. (b) Taylor, D. *Aust. J. Chem.* **1978**, *31*, 713. (c) Jin, S.; Nieuwenhuyzen, M.; Wilkins, C. J. *J. Chem. Soc., Dalton Trans.* **1992**, 2071. (d) Wood, J. S. *Inorg. Chim. Acta* **1995**, *229*, 407.

**Table 3.** Selected Interatomic Distances (Å) and Angles (deg) in the Cation of **3**, $[Ni_4(LH)_3]^{2+}$

| | | | |
|---|---|---|---|
| Ni(1)−N(4) | 2.034(7) | Ni(1)−O(6)−Ni(2) | 113.5(2) |
| Ni(1)−O(6) | 2.040(4) | Ni(1)−O(6)−N(6) | 121.6(3) |
| Ni(1)−N(5) | 2.064(6) | Ni(2)−O(4)−N(4) | 113.5(4) |
| Ni(1)−N(1) | 2.065(7) | Ni(2)−O(6)−N(6) | 113.2(3) |
| Ni(1)−N(3) | 2.078(6) | | |
| Ni(1)−N(2) | 2.120(7) | | |
| Ni(2)−O(4) | 2.044(5) | | |
| N(4)−C(12) | 1.284(10) | | |
| N(4)−O(4) | 1.358(8) | | |
| N(5)−C(22) | 1.259(12) | | |
| N(5)−O(5) | 1.390(9) | | |
| N(6)−C(32) | 1.289(8) | | |
| N(6)−O(6) | 1.373(7) | | |
| N(4)−Ni(1)−O(6) | 88.6(2) | O(4)−Ni(2)−O(4)#1 | 85.9(2) |
| N(4)−Ni(1)−N(5) | 100.1(3) | O(4)−Ni(2)−O(4)#2 | 85.9(2) |
| O(6)−Ni(1)−N(5) | 91.3(2) | O(4)−Ni(2)−O(6)#2 | 174.2(2) |
| N(4)−Ni(1)−N(1) | 81.2(3) | O(4)#1−Ni(2)−O(6)#2 | 92.8(2) |
| O(6)−Ni(1)−N(1) | 167.9(3) | O(4)#2−Ni(2)−O(6)#2 | 88.3(2) |
| N(5)−Ni(1)−N(1) | 96.8(3) | O(4)−Ni(2)−O(6) | 88.3(2) |
| N(4)−Ni(1)−N(3) | 96.7(3) | O(4)#1−Ni(2)−O(6) | 174.1(2) |
| O(6)−Ni(1)−N(3) | 90.1(2) | O(4)#2−Ni(2)−O(6) | 92.8(2) |
| N(5)−Ni(1)−N(3) | 163.1(3) | O(6)#2−Ni(2)−O(6) | 92.9(2) |
| N(1)−Ni(1)−N(3) | 84.7(3) | O(4)−Ni(2)−O(6)#1 | 92.8(2) |
| N(4)−Ni(1)−N(2) | 164.5(2) | O(4)#1−Ni(2)−O(6)#1 | 88.3(2) |
| O(6)−Ni(1)−N(2) | 106.7(2) | O(4)#2−Ni(2)−O(6)#1 | 174.2(2) |
| N(5)−Ni(1)−N(2) | 77.9(3) | O(6)#2−Ni(2)−O(6)#1 | 92.9(2) |
| N(1)−Ni(1)−N(2) | 83.8(3) | O(6)−Ni(2)−O(6)#1 | 92.9(2) |
| N(3)−Ni(1)−N(2) | 85.6(3) | | |

graphically equivalent nickel(II) centers, Ni(1). The Ni(1) center is coordinated to three macrocyclic amine nitrogens N(1), N(2), and N(3), two azomethine nitrogens N(4) and N(5), and an oximato O(6), thus attaining a six-coordinated $NiN_5O$ core. The three pendent oximic groups (C═N−OH) of the ligand act in three different ways: (i) a protonated nonbridging >C═N−OH group, which is virtually the universal bonding mode for oximes, (ii) a two-atom (N−$O^-$) bridging group between two metal centers, as usual, and (iii) a monatomic oximato-O,O(6) bridging. That an oxime group acts as a bridging ligand only through the oxygen atom is still a matter of curiosity;[5f,50] this monatomic oxygen bridging leads to a six-membered ring comprising Ni(1)N(3)C(31)C(32)N(6)O(6).

Thus the complex cation in **3** can also be described as three $[NiLH]^0$ units acting as bidentate ligands for the central Ni(2) yielding the $NiO_6$ core. The configuration at both Ni(1) and Ni(2) centers is Δ. The Ni(1)···Ni(2) distance of 3.475(1) Å is comparable to the value reported for similar oximic monatomic O-bridged compounds.[50b] The intramolecular Ni(1)···Ni(1A) separation is 6.016(2) Å.

The Ni(1) is bonded to four atoms N(1), N(3), O(6), and N(5), comprising the equatorial plane. The apically situated Ni(1)−N(2)(amine) bond is appreciable longer, 2.120(7) Å, than the other comparable Ni(1)−N bond lengths, av 2.07(2) Å, as has been observed[23−27] for the tacn and its derivatives earlier. The geometry at Ni(1) is distorted from octahedral, the cis bond angles are in the range 77.9(3)−106.7(2)°, while the trans angles vary from 163.1(3) to167.9(3)°. The angle O(6)−Ni(1)−N(2) is 106.7(2)°. The Ni(1)−N(amine) distances are slightly longer (av 2.088 ± 0.03 Å) than the Ni(1)−N(oxime) distances (av 2.049 ± 0.015 Å). There is no discernible difference between the Ni(1)−O(6)(oxime), 2.040(4) Å, and Ni(1)−N(4)(oxime) and Ni(1)−N(5)(oxime) distances, 2.034(7) and 2.064(6) Å, respectively.

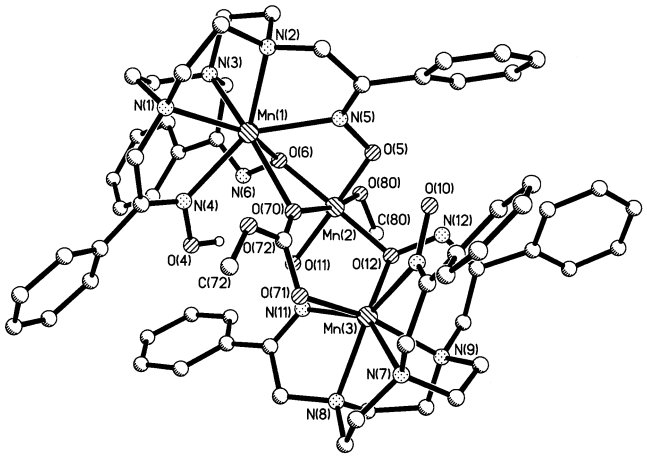


**Figure 4.** Structure of the cation $[L_2Mn^{II}_2(\mu_2\text{-}O_2COCH_3)(CH_3OH)Mn^{III}]^{2+}$ in the crystal of **4** with the atom-numbering scheme.

The coordination geometry of Ni(2) deviates also from octahedron, with two different Ni(2)−O bond lengths, 2.044(5) and 2.115(4) Å. The four equatorially coordinating atoms O(6), O(6A), O(4A), and O(4B) of Ni(2) are nearly coplanar with the deviation of 0.041 Å, and the Ni(2) atom is located on the mean plane with a deviation of 0.062 Å. The bridging Ni(2)O(4)N(4)Ni(1) and Ni(2)O(6)N(6)Ni(1) units are not planar. A hydrogen bond can be envisaged between the protonated O(5) and O(4A), 2.541(5) Å. The interligand bonding parameters are unremarkable and are comparable with those reported for other complexes with tacn derivatives.[26,27]

**X-ray Structure of $[L_2Mn^{II}_2(\mu\text{-}O_2COCH_3)(CH_3OH)Mn^{III}](ClO_4)_2\cdot 2CH_3OH\cdot 3H_2O$ (4).** Figure 4 shows the atom-labeling scheme and the molecular geometry of the cation in **4**. Table 4 lists relevant bond distances and angles. The structure is unusual because the Mn(II) centers, Mn(1) and Mn(3), are coordinated to seven donor atoms arising from oxygens of a bridging monomethyl carbonato, from oxygens and nitrogens of two oxime ligands L. A perspective view of the core structure is shown in Figure 5. A mixed-valence compound $Mn^{II}Mn^{III}Mn^{II}$ with two terminals Mn(II), Mn(1), and Mn(3) and one central Mn(III), Mn(2) is evident from the bond lengths and the susceptibility measurements described later.

The Mn(1) center is coordinated to three macrocyclic amine nitrogens, N(1), N(2), and N(3), two azomethine nitrogens, N(4) and N(5), and two bridging oxygens (O(6) of an oximato group and O(70) of the monomethyl carbonato group), thus attaining a seven-coordinated $MnN_5O_2$ core. Mn(1) has an idealized pentagonal-bipyramidal geometry with N(1)N(2)O(6)N(5)N(4) comprising the equatorial plane. The axial angle O(70)−Mn(1)−N(3) of 155.2(3)° is substantially smaller than the expected 180°. Three pendent oximic groups

(50) (a) Ruiz, R.; Sanz, J.; Lloret, F.; Julve, M.; Fans, J.; Bois, C.; Munoz, M. C. *J. Chem. Soc., Dalton Trans.* **1993**, 3035. (b) Colacio, E.; Dominguez-Vera, J. M.; Escuer, A.; Kivekas, R.; Romerosa, A. *Inorg. Chem.* **1994**, *33*, 3914. (c) Gouzerh, P.; Jeanin, P.; Rocchiccioli-Deltcheff, C.; Valentini, F. *J. Coord. Chem.* **1979**, *9*, 221.

**Table 4.** Selected Bond Lengths (Å) and Angles (deg) for $[L_2Mn^{II}_2(\mu\text{-}O_2COCH_3)\text{-}(CH_3OH)Mn^{III}](ClO_4)_2\cdot 2CH_3OH\cdot 3H_2O$ **4**

| | | | |
|---|---|---|---|
| Mn(1)−O(6) | 2.177(5) | O(6)−Mn(1)−O(71X) | 117.1(4) |
| Mn(1)−O(71X) | 2.24(2) | O(6)−Mn(1)−N(5) | 73.9(2) |
| Mn(1)−N(5) | 2.292(7) | O(71X)−Mn(1)−N(5) | 84.2(5) |
| Mn(1)−O(70) | 2.314(9) | O(6)−Mn(1)−O(70) | 77.1(2) |
| Mn(1)−N(2) | 2.316(7) | N(5)−Mn(1)−O(70) | 69.7(3) |
| Mn(1)−N(3) | 2.334(7) | O(6)−Mn(1)−N(2) | 125.2(2) |
| Mn(1)−N(1) | 2.339(6) | O(71X)−Mn(1)−N(2) | 98.4(4) |
| Mn(1)−N(4) | 2.361(6) | N(5)−Mn(1)−N(2) | 69.5(2) |
| Mn(2)−O(5) | 1.899(5) | O(70)−Mn(1)−N(2) | 123.2(3) |
| Mn(2)−O(11) | 1.905(5) | O(6)−Mn(1)−N(3) | 79.0(2) |
| Mn(2)−O(6) | 1.913(5) | O(71X)−Mn(1)−N(3) | 161.7(4) |
| Mn(2)−O(12) | 1.922(5) | N(5)−Mn(1)−N(3) | 109.9(2) |
| Mn(2)−O(80) | 2.189(5) | O(70)−Mn(1)−N(3) | 155.2(3) |
| Mn(2)−O(70) | 2.351(8) | N(2)−Mn(1)−N(3) | 76.9(2) |
| Mn(2)−O(70X) | 2.358(13) | O(6)−Mn(1)−N(1) | 142.8(2) |
| Mn(3)−O(12) | 2.165(5) | O(71X)−Mn(1)−N(1) | 84.8(4) |
| Mn(3)−O(71) | 2.192(8) | N(5)−Mn(1)−N(1) | 141.4(2) |
| Mn(3)−N(11) | 2.266(7) | O(70)−Mn(1)−N(1) | 119.8(3) |
| Mn(3)−O(70X) | 2.30(2) | N(2)−Mn(1)−N(1) | 75.7(2) |
| Mn(3)−N(7) | 2.301(7) | N(3)−Mn(1)−N(1) | 76.9(2) |
| Mn(3)−N(8) | 2.341(6) | O(6)−Mn(1)−N(4) | 85.8(2) |
| Mn(3)−N(9) | 2.353(7) | O(71X)−Mn(1)−N(4) | 76.7(5) |
| Mn(3)−N(10) | 2.387(7) | N(5)−Mn(1)−N(4) | 141.9(2) |
| | | O(70)−Mn(1)−N(4) | 74.6(3) |
| N(11)−Mn(3)−N(8) | 70.1(2) | N(2)−Mn(1)−N(4) | 145.4(2) |
| O(70X)−Mn(3)−N(8) | 124.7(4) | N(3)−Mn(1)−N(4) | 97.0(2) |
| N(7)−Mn(3)−N(8) | 76.3(2) | N(1)−Mn(1)−N(4) | 69.7(2) |
| O(12)−Mn(3)−N(9) | 79.7(2) | O(5)−Mn(2)−O(11) | 168.3(2) |
| O(71)−Mn(3)−N(9) | 162.5(3) | O(5)−Mn(2)−O(6) | 89.4(2) |
| N(11)−Mn(3)−N(9) | 109.7(2) | O(11)−Mn(2)−O(6) | 90.8(2) |
| | | O(5)−Mn(2)−O(12) | 92.0(2) |
| O(70X)−Mn(3)−N(9) | 154.2(4) | O(11)−Mn(2)−O(12) | 87.9(2) |
| N(7)−Mn(3)−N(9) | 76.6(2) | O(6)−Mn(2)−O(12) | 178.4(2) |
| N(8)−Mn(3)−N(9) | 76.0(2) | O(5)−Mn(2)−O(80) | 99.4(2) |
| O(12)−Mn(3)−N(10) | 84.7(2) | O(11)−Mn(2)−O(80) | 92.3(2) |
| O(71)−Mn(3)−N(10) | 78.9(3) | O(6)−Mn(2)−O(80) | 88.7(2) |
| N(11)−Mn(3)−N(10) | 140.7(2) | O(12)−Mn(2)−O(80) | 90.3(2) |
| O(70X)−Mn(3)−N(10) | 73.6(4) | O(5)−Mn(2)−O(70) | 80.2(3) |
| N(7)−Mn(3)−N(10) | 70.2(2) | O(11)−Mn(2)−O(70) | 88.3(3) |
| N(8)−Mn(3)−N(10) | 146.4(2) | O(6)−Mn(2)−O(70) | 81.4(3) |
| N(9)−Mn(3)−N(10) | 97.5(2) | O(12)−Mn(2)−O(70) | 99.6(3) |
| Mn(1)−O(70)−Mn(2) | 89.3(2) | O(80)−Mn(2)−O(70) | 170.1(3) |
| Mn(2)−O(6)−Mn(1) | 106.3(3) | O(5)−Mn(2)−O(70X) | 88.9(4) |
| Mn(2)−O(12)−Mn(3) | 108.6(2) | O(11)−Mn(2)−O(70X) | 79.7(4) |
| Mn(2)−O(11)−N(11) | 113.2(2) | | |
| Mn(3)−N(11)−O(11) | 121.8(2) | O(6)−Mn(2)−O(70X) | 102.3(4) |
| Mn(2)−O(5)−N(5) | 112.8(2) | O(12)−Mn(2)−O(70X) | 78.6(4) |
| Mn(1)−N(5)−O(5) | 120.1(2) | O(80)−Mn(2)−O(70X) | 166.4(4) |
| Mn(1)···Mn(2) | 3.278(2) | O(12)−Mn(3)−O(71) | 116.6(2) |
| Mn(2)···Mn(3) | 3.321(2) | O(12)−Mn(3)−N(11) | 73.2(2) |
| Mn(3)···Mn(1) | 5.442(3) | O(71)−Mn(3)−N(11) | 82.5(3) |
| | | O(12)−Mn(3)−O(70X) | 75.4(3) |
| | | N(11)−Mn(3)−O(70X) | 69.6(4) |
| | | O(12)−Mn(3)−N(7) | 142.4(2) |
| | | O(71)−Mn(3)−N(7) | 86.2(3) |
| | | N(11)−Mn(3)−N(7) | 142.6(2) |
| | | O(70X)−Mn(3)−N(7) | 120.5(4) |
| | | O(12)−Mn(3)−N(8) | 125.2(2) |
| | | O(71)−Mn(3)−N(8) | 97.4(3) |

(>C═N−OH) of the ligand L act in three different ways, as has been observed also in **3**, and will not be discussed here again. The monatomic oximato-O donors, O(6) and O(12), bridge the metal centers Mn(1) and Mn(2), and, Mn(2) and Mn(3), respectively. This monatomic oximic-oxygen bridging leads to two six-membered rings comprising Mn(1)O(6)N(6)C(24)C(23)N(3) and Mn(3)O(12)N(12)C(54)C(53)N(9). The usual coordination number of Mn(II) is 6, and since high-spin Mn(II) obtains no ligand field stabilization in either an octahedral or tetrahedral environment, the geometry about the Mn is dictated by the ligand constraints.

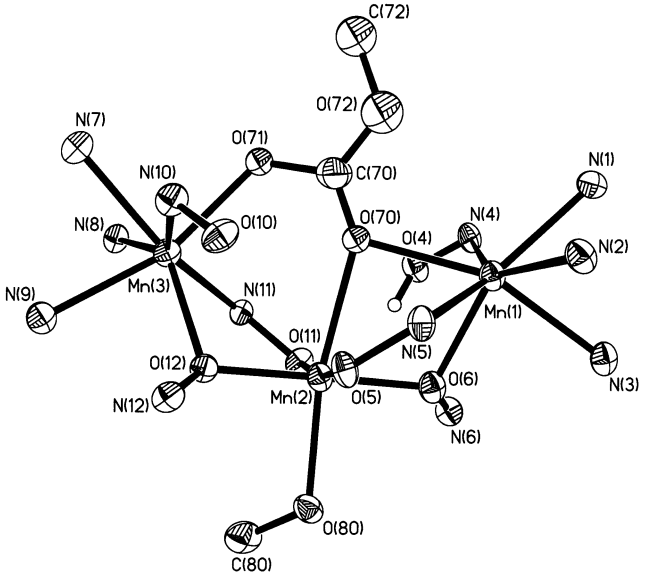


**Figure 5.** The first coordination sphere of the cation containing the trinuclear manganese centers $[Mn^{II}Mn^{III}Mn^{II}]$ in **4**.

In this case, we observe a seven-coordinated Mn(II) with close to pentagonal-bipyramidal geometry.

A very similar coordination environment is attained by the manganese center Mn(3) with O(2)N(11)N(7)N(8)N(10) as the equatorial plane. The two terminal centers, Mn(1) and Mn(3), have essentially the same coordination geometry $MnN_5O_2$ with average Mn−O,N bond distances of 2.212 and 2.329 Å, respectively, consistent with previously reported typical Mn(II)−O,N distances.[5,51]

The coordination geometry of the central Mn(2) ion is distorted octahedral with six oxygen donor atoms (Figure 5), oxime O(6), O(5), O(11) and O(12), O(80) from a methanol molecule and O(70) of the bridging monomethyl carbonate. That Mn(2) is a Jahn−Teller distorted high-spin $d^4$ Mn(III) ion is clearly shown by the X-ray structure; the axially elongated sites are occupied by the carboxylate oxygen atom O(70) of the monomethyl carbonate group and O(80) from a methanol molecule, with Mn(2)−O(70) 2.351(8) Å, Mn(2)−O(80) 2.189(5) Å, and O(70)−Mn(2)−O(80) 170.1(3)°.

The monomethyl carbonate ion plays the role of a bridging ligand, linking all three manganese centers. Notably O(70) acts as a monatomic bridging ligand between Mn(1) and Mn(2), whereas the second oxygen O(71) of the carboxylate group is a donor atom only for Mn(3).

The three manganese ions are not linearly situated with an angle of 111.1° for Mn(1)−Mn(2)−Mn(3). The Mn(1)···Mn(2), Mn(2)···Mn(3), and Mn(1)···Mn(3) distances are 3.278(2), 3.321(2), and 5.442(3) Å, respectively.

Thus the very rare mixed-valence state $Mn^{II}Mn^{III}Mn^{II}$ of the cation in **4** is unambiguously proved by the X-ray structure determination. It is noteworthy that in contrast to relatively common $Mn^{III}_3$ and $Mn^{III}Mn^{II}Mn^{III}$ trimanganese

(51) (a) Unni Nair, B. C.; Sheats, J. E.; Ponteciello, R.; Van Eugen, D.; Petrouleas, V.; Dismukes, G. C. *Inorg. Chem.* **1989**, *28*, 1582. (b) Jurisson, S.; Francesconi, L.; Linder, K. E.; Treher, E.; Malley, M. F.; Gougoutas, J. Z.; Nunn, A. D. *Inorg. Chem.* **1991**, *30*, 1820.

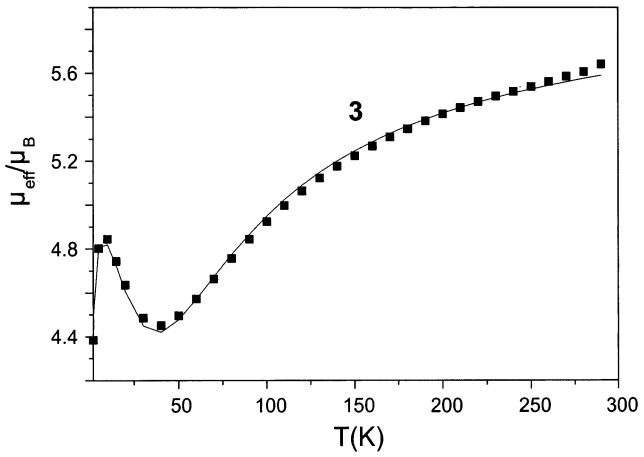


**Figure 6.** Plot of $\mu_{eff}$ vs $T$ for solid **3**. The solid line represents the best fit with the full-diagonalization matrix method.

systems,[14a,52] the cation in **4** with $Mn^{II}Mn^{III}Mn^{II}$ represents a rare case of the mixed-valence trinuclear manganese complex. A very similar mixed-valence trinuclear $Mn^{II}Mn^{III}$-$Mn^{II}$ system of class I type in the Robin−Day classification recently has been reported[53] in the cavity of a large macrocyclic ligand, in which in contrast to **4** all three manganese centers have the same coordination geometry of distorted octahedron.

**Magnetic Susceptibility Measurements.** Variable-temperature (2−290 K) magnetic susceptibility data were collected for **1**, **3**, and **4**. The magnetic moments of 1.69 $\mu_B$ at 5 K and 1.73 $\mu_B$ at 290 K for complex **1** indicate clearly that copper in complex **1** is in the oxidation state +II. As **2** was not obtained in pure form, magnetic susceptibility data could not be collected. Hence, only the structure is discussed. Complex **2a** is diamagnetic, showing that all three cobalt centers are in low-spin $d^6$ electron configurations.

The magnetic properties of **3** were studied in the range 2−290 K and the results are given in Figure 6 in the form of a plot of $\mu_{eff}$ vs $T$. The magnetic moment at 290 K is 5.56 $\mu_B$ ($\chi_M \cdot T = 3.858$ cm$^3$ mol$^{-1}$ K), which is slightly smaller than the spin-only value of 5.66 $\mu_B$, calculated from the expression $\mu_{eff}^2 = 4\,\mu_{Ni}^2$ with $\mu_{Ni} = 2.83\,\mu_B$. On lowering the temperature, $\mu_{eff}$ decreases monotonically approaching a broad minimum around 30−50 K with $\mu_{eff} \sim 4.42\,\mu_B$ ($\chi_M \cdot T = 2.445$ cm$^3$ mol$^{-1}$ K), and increases upon further cooling. The temperature behavior of the magnetic moment of **3** clearly indicates an antiferromagnetic coupling between the $S = 1.0$ of Ni(II) centers. The magnetic moment $\mu_{eff}$ reaches at 10 K a maximum value of 4.82 $\mu_B$ ($\chi_M \cdot T = 2.907$ cm$^3$ mol$^{-1}$ K), which is very close to the value of 4.90 $\mu_B$ for a hypothetically isolated $S = 2.0$. An $S_t = 2.0$ state is expected as the ground state resulting from antiferromagnetic interactions between three Ni(II) centers ($S_{Ni} = 1.0$) arranged in an equivalent triangle and a Ni(II) ion present at the center of the triangle. Below 10 K there is a decrease in $\mu_{eff}$ for **3**, which reaches a value of 4.37 $\mu_B$ at 2 K; this behavior might be attributed to the splitting in zero-field of the ground state and intermolecular interactions.

**Scheme 1**

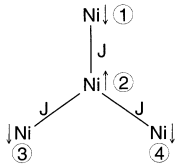


The experimental magnetic data were simulated by using a least-squares-fitting computer program with a full-matrix diagonalization approach including exchange coupling, Zeeman splitting, and single-ion zero-field splitting. Given the large distance of 6.0 Å between the peripheral Ni atoms, Ni(1), and its equivalents (Figure 3), the interactions between them can be safely neglected, and only one exchange coupling constant $J = J_{12} = J_{23} = J_{24}$ is required for describing the exchange interactions between the nickel centers in **3**. Thus the spin Hamiltonian in use to describe the isotropic exchange interactions in Scheme 1 is given by

$$\hat{H} = -2J(\hat{S}_1 \cdot \hat{S}_2 + \hat{S}_2 \cdot \hat{S}_3 + \hat{S}_2 \cdot \hat{S}_4)$$

where $S_i$ ($i = 1, 2, 3, 4$) $= 1.0$. The correspondingly calculated (Figure 6, solid line) $\mu_{eff}$ vs $T$ curve, with $J = -13.4$ cm$^{-1}$, $g_{Ni(central)} = 2.271$, and $g_{Ni(peripheral)} = 2.055$, shows very good agreement with the experimental data. No other terms were used for the simulation shown in Figure 6.

The broad minimum at 30−50 K with $\mu_{eff} \sim 4.42\,\mu_B$ in Figure 6 can be readily understood if one considers the low-lying spin ladder above the ground state $|S_t = 2.0, S_{134} = 3\rangle$. With use of the evaluated exchange coupling constant of $J = -13.4$ cm$^{-1}$, the first and second excited states are found to be $|S_t = 1.0, S_{134} = 2\rangle$ and $|S_t = 0.0, S_{134} = 1\rangle$, respectively, which lie 26.8 and 53.6 cm$^{-1}$ above the ground state with $S_t = 2.0$. Since the total spin of the first and second excited states is $S_t = 1.0$, and 0, their population with increasing temperature reduces the effective magnetic moment of **3**. Population of the third excited state with $S_t = 3.0$ occurs above ∼50 K, which accounts for the increase in $\mu_{eff}$ at higher temperatures. As a result a minimum is observed in the magnetic moment curve.

We have confirmed the ground state of **3** ($[Ni_4(LH)_3](ClO_4)_2$) to be $S_t = 2.0$ by performing the magnetization measurements at different applied magnetic fields of 1, 4, and 7 T. The field-dependent magnetization as a function of temperature and their simulations are depicted in Figure 7. The simulated parameters are $S = 2.0$ (fixed), $g = 2.0$, and $D = 0.65$ cm$^{-1}$. We recall that one should not put too much significance on the sign and values of $D$ evaluated through the fitting procedure of powder susceptibility data.[18] The data at different magnetic fields are practically superimposable, indicating a very small ZFS parameter.

On the basis of the existing body of results on the exchange-coupled mixed-bridged Ni(II) complexes, the major

(52) (a) Kessissoglou, D. P.; Kirk, M. L.; Lah, M. S.; Li, X.; Raptopoulou, C.; Hatfield, W. E.; Pecoraro, V. L. *Inorg. Chem.* **1992**, *31*, 5424. (b) Tangoulis, V.; Malamatari, D. A.; Spyroulias, G. A.; Raptopoulou, C. P.; Terzis, A.; Kessissoglou, D. P. *Inorg. Chem.* **2000**, *39*, 2621 and references therein. (c) Hirotsu, M.; Kojima, M.; Yoshikawa, Y. *Bull. Chem. Soc. Jpn.* **1997**, *70*, 649.

(53) Yoshino, A.; Miyagi, T.; Asato, E.; Mikuriya, M.; Sakata, Y.; Sugiura, K.; Iwasaki, K.; Hino, S. *Chem. Commun.* **2000**, 1475.

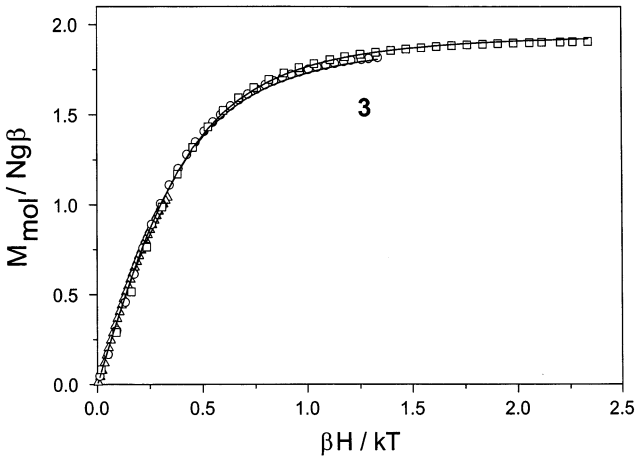


**Figure 7.** Plots of the reduced magnetization M/(Ng$\beta$) vs $\beta$H/kT for **3**. Fields are 1, 4, and 7 T. Solid lines are the theoretical curves.

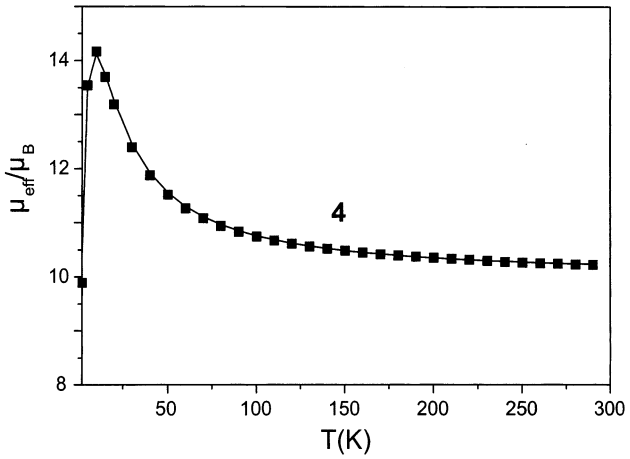


**Figure 8.** $\mu_{eff}$ of solid **4** as a function of temperature. The solid line represents the best fit of the data to the theoretical model.

contributor to the superexchange constants is considered to be the Ni−O−Ni angle.[56] The angle Ni(1)−O(6)−Ni(2) being 113.5° for **3** is consonant with the antiferromagnetic spin coupling with $J = -13.4$ cm$^{-1}$, which is comparable with those values reported for comparable compounds.[57] This moderate coupling is consistent with its mediation by two types of oximate bridges, a single-atom O-bridge and a two-atom N−O linkage, of which the latter's contribution is expected to be small.

We want to emphasize that the magnetic analysis of **3** unambiguously demonstrates the antiferromagnetic nature of the exchange interactions yielding the ground-state $S_t = 2.0$ owing to the topology of spin-carriers in **3**, as shown in Scheme 1. A ferromgnetic-like behavior is obtained with a ground state characterized by a large spin, although the interaction between nearest neighbor Ni$^{II}$ ions ($S_{Ni} = 1.0$) is antiferromagnetic in a planar trigonal-shaped tetranuclear Ni(II) species **3**. A simple one-$J$ Heisenberg Hamiltonian approach, ignoring any edge interactions, can adequately describe the exchange interactions in **3**. This effective ferromagnetic coupling between the peripheral ions is highly interesting in the context of synthesizing "high-spin" molecules.

The magnetic moment $\mu_{eff}$ vs $T$ plot with an applied field of 1 T for **4** in the range 2−290 K is shown in Figure 8. The magnetic moment at 290 K is 10.18 $\mu_B$ ($\chi_M \cdot T = 12.96$ cm$^3$ mol$^{-1}$ K), which is significantly greater than the spin-only value of 9.71 $\mu_B$ for two high-spin Mn(II) and one high-spin Mn(III) ions. On lowering the temperature, $\mu_{eff}$ increases monotonically reaching at 10 K a maximum value of 14.11 $\mu_B$ ($\chi_M \cdot T = 24.88$ cm$^3$ mol$^{-1}$ K), which is close to the value of 14.97 $\mu_B$ for a hypothetically isolated $S = 7.0$ with $g = 2.0$. An $S_t = 7.0$ value is expected as the ground state resulting from ferromagnetic interactions between three spins of $S = {}^5/_2$, 2.0, and ${}^5/_2$ arranged in a linear fashion. Below

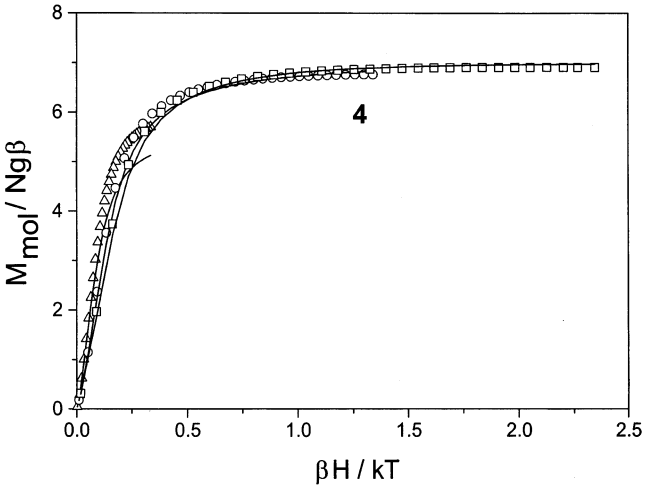


**Figure 9.** Reduced magnetization curves for **4** at applied fields of 1, 4, and 7 T. The solid lines represent the best fit with the full-diagonalization matrix method.

10 K there is a decrease in $\mu_{eff}$ for **4**, which reaches a value of 10.24 $\mu_B$ at 2 K.

The data suggest a large ground-state spin value, which can be determined by examining the magnetization of the compound at low temperatures as a function of the applied magnetic fields. We have performed magnetization measurements at applied magnetic fields of 1, 4, and 7 T and collected most of the magnetization data in the temperature range 2.00−10.3 K (26 data point) and only 7 data points in the range 12.3−260.0 K, which are shown in Figure 9 as plots of M/Ng$\beta$ vs $\beta$H/kT.

The data sets at different magnetic fields are nearly superimposable, particularly data for 4 and 7 T, indicating the presence of very small zero-field splitting (ZFS) in the ground state, if at all. From Figure 9 it is clear that the magnetization value tends to 7 (the highest experimental value is 6.77 at the highest field, 7 T). This reduced magnetization is very close to saturation under these conditions. The value 6.77 is consistent with the $S_t = 7.0$ ground state and a $g$ value less than 2, as expected for manganese. This value is not consistent with an $S_t = 6.0$ ground state. The simulated parameters are $J = +2.0$ cm$^{-1}$, $g = 2.0$

(54) Lloret, F.; Journaux, Y.; Julve, M. *Inorg. Chem.* **1990**, *29*, 3967.
(55) Schake, A. R.; Schmitt, E. A.; Conti, A. J.; Streib, W. E.; Huffman, J. C.; Hendrickson, D. N.; Christou, G. *Inorg. Chem.* **1991**, *30*, 3192.
(56) Halcrow, M. A.; Sun, J. S.; Huffman, J. C.; Christou, G. *Inorg. Chem.* **1995**, *34*, 4167 and references therein.
(57) Pavlishchuk, V. V.; Kolotilov, S. V.; Addison, A. W.; Prushan, M. J.; Butcher, R. J.; Thompson, L. K. *Inorg. Chem.* **1999**, *38*, 1759.

(fixed), and $D = 0.6$ cm$^{-1}$. The quality of fit, shown in Figure 9, particularly for 1 T, is not very satisfactory. We conclude that in the 2−4 K range, the lowest energy state in a 1−7 T field has $S_t = 7$. At temperatures above ca. 4 K, other states with smaller $S$ values are presumably populated and this is why the maximum in $\mu_{eff}$ ($H = 1$ T) at ca. 10 K falls short of the value expected for a molecule with $S = 7$; weak, intermolecular antiferromagnetic exchange interactions likely also serve to decrease the $\mu_{eff}$ value at low temperatures.

The susceptibility of [$Mn^{II}Mn^{III}Mn^{II}$], **4**, was calculated by using a full-matrix diagonalization approach of the spin Hamiltonian

$$H = -2J(\hat{S}_1 \cdot \hat{S}_2 + \hat{S}_2 \cdot \hat{S}_3) - 2J_{13}(\hat{S}_1 \cdot \hat{S}_3)$$

with $S_1 = S_3 = {}^5/_2$ and $S_2 = {}^4/_2$. Considering the large distance of ~6.0 Å between the terminal Mn(II) ions, $J_{13}$, describing the spin interaction between the terminal ions within the trinuclear complex **4**, was kept fixed at zero. The agreement between the calculated and observed magnetic moments is excellent and the best fit is shown as a solid line in Figure 8. The best fit parameters are $J = +2.0$ cm$^{-1}$, $g_1 = g_3 = 2.05$, $g_2 = 1.98$, and TIP $= 360 \times 10^{-6}$ cm$^3$ mol$^{-1}$. No paramagnetic impurity was needed for the simulation shown in Figure 8. As the two other conceivable models, $J_{12} \neq J_{23} \neq J_{13}$ and $J_{12} \neq J_{23}$, $J_{13} = 0$, do not yield better fits, we have preferred the simplest model and avoided overparametrization. Thus we conclude that the exchange interaction prevailing between the neighboring high-spin Mn(II) and high-spin Mn(III) ions is of ferromagnetic nature leading to a ground state of $S_t = 7.0$ for **4**.

The exchange coupling in **4** is mediated mainly by two types of bridges, a single-atom O-bridge and a two-atom N−O linkage, of which the latter's contribution is expected to be small. The angle at the bridging oxygen would be expected to be important, for this affects the nature of $\sigma$ and $\pi$ overlap between the metal magnetic orbitals and the oxygen $p_x$, $p_y$, and $p_z$ orbitals that mediate the exchange. The bridging angle Mn(1)−O(70)−Mn(2) in **4** of 89.3° is smallest among the Mn−O−Mn angles (96.6° and 107.7°; 97.1° and 102.4°) in two other ferromagnetically coupled $Mn^{II}$−$Mn^{III}$ compounds.[53,55] The smaller Mn−O−Mn angles would be expected to increase the contribution to $J$ from ferromagnetic pathways, due to the near orthogonality of some of the magnetic orbitals. Thus the net ferromagnetic coupling in **4** is noticeably stronger than that of the other two compounds. It must be pointed out that the net exchange interaction in a $d^4$(h.s.)/$d^5$(h.s.) system is expected to be weak.

## Concluding Remarks

The pendent-arm ligand 1,4,7-tris(acetophenoneoxime)-1,4,7-triazacyclononane forms stable polynuclear complexes with transition metals in oxidation states II and III. The coordination number is dependent on the metal center, varying between 6 and 7. A notable point is the formation of a bridging monomethyl carbonato ligand through spontaneous carbondioxide uptake from air by methanolic solutions containing $NEt_3$ as a base. The oxime part of the ligand stabilizes as expected the +2 oxidation state of manganese.

The results described in the present paper show that it is possible to stabilize a high-spin ground state, despite antiferromagnetic interactions prevailing between the spin carriers, due to the molecular topology of the paramagnetic centers.[54] Complex **3**, a planar trigonal-shaped tetranuclear Ni(II) species, exhibits an irregular spin-level structure.[18]

Complex **4**, a trinuclear manganese complex, is one of a few examples[53,55] of ferromagnetic coupling prevailing between high-spin Mn(II) and high-spin Mn(III), thus resulting in a molecule with a ground state of $S_t = 7.0$. It is tempting at this point to anticipate a tetranuclear complex with the topology of **3**, but with Mn(II) as peripheral ions and Mn(III) as the central ion. This molecule would exhibit a ground state of $S_t = {}^{19}/_2$!! We are trying to synthesize such a molecule by using similar pendent-arm oxime functionality.

## Experimental Section

**Materials and Physical Measurements.** Reagent or analytical grade materials were obtained from commercial suppliers and used without further purification, unless otherwise stated. The macrocycle 1,4,7-triazacyclononane ($C_6H_{15}N_3$, TACN) was prepared[46] according to a modification of the method described by Atkins et al.[47] Fourier transform infrared spectroscopy on KBr pellets was performed on a Perkin-Elmer 2000 FT-IR instrument. Solution electronic spectra were measured on a Perkin-Elmer Lambda 19 spectrophotometer. Mass spectra were recorded either in the EI or ESI positive (in $CH_3CN$) mode with a Finnigan MAT 95 or 8200 spectrometer. Magnetic susceptibilities of the polycrystalline samples were recorded on a SQUID magnetometer (MPMS, Quantum Design) in the temperature range 2−290 K with an applied field of 1 T. Experimental susceptibility data were corrected for the underlying diamagnetism by using Pascal's constants.

**X-ray Crystallographic Data Collection and Refinement of the Structures.** Single crystals of **1** (deep blue), **2** (red-orange), **3** (yellow-brown), and **4** (black-brown) were coated with perfluoropolyether, picked up with glass fibers, and mounted on Kappa-CCD diffractometers equipped with a nitrogen cold stream at 100 K. Graphite-monochromated Mo Kα radiation ($\lambda = 0.71073$ Å) was used. Crystallographic data of the compounds and diffractometer types used are listed in Table 5. Cell constants were obtained from a least-squares fit of the diffraction angles of several thousand strong reflections. Intensity data were corrected for Lorentz and polarization effects. Data sets of **1**, **2**, and **3** were corrected for absorption with use of the programs SADABS, MulScanAbs, and DelRefAbs, respectively, whereas the intensities of **4** were left uncorrected. The Siemens ShelXTL software package (G. M. Sheldrick, Universität Göttingen) was used for solution, refinement, and artwork of the structures, and neutral atom scattering factors of the program were used. All structures were solved and refined by direct methods and difference Fourier techniques. Non-hydrogen atoms were refined anisotropically, and hydrogen atoms were placed at calculated positions and refined as riding atoms with isotropic displacement parameters. The monomethyl carbonate group in **4** was found to be disordered and a split model was applied.

**Ligand Synthesis: ω-Chloroacetophenoneoxime.** To a slurry of ω-chloroacetophenone (30.0 g; 0.194 mmol) and hydroxylamine hydrochloride (40.4 g; 0.582 mmol) in 40 mL of water was added with stirring portionwise methanol (~300 mL) to yield a clear solution. The clear solution was stirred overnight at room temperature and added to 400 mL of water, whereupon a white solid precipitated out. The oxime product was filtered out, washed several

**Table 5.** Crystallographic Data for $[LH_2Cu^{II}]ClO_4 \cdot 0.5\ Et_2O$ (**1**), $[L_2Co^{III}_2Co^{II}](ClO_4)_2 \cdot H_2O \cdot Et_2O \cdot Me_2Co$ (**2**), $[(LH)_3Ni^{II}_4](ClO_4)_2 \cdot 3H_2O$ (**3**), and $[L_2Mn^{II}_2(\mu\text{-}O_2COMe)(MeOH)Mn^{III}](ClO_4)_2 \cdot 2MeOH \cdot 3H_2O$ (**4**)

| | $Cu^{II}$ **1** | $Co^{III}_2Co^{II}$ **2** | $Ni^{II}_4$ **3** | $Mn^{II}_2Mn^{III}$ **4** |
|---|---|---|---|---|
| formula | $C_{30}H_{35}ClCuN_6O_7 \cdot CH_3OH$ | $C_{67}H_{86}Cl_2Co_3N_{12}O_{18}$ | $C_{90}H_{108}Cl_2N_{18}Ni_4O_{20}$ | $C_{65}H_{89}Cl_2Mn_3N_{12}O_{23}$ |
| fw | 722.69 | 1595.17 | 2067.68 | 1642.20 |
| $T$ (K) | 100(2) | 100(2) | 100(2) | 100(2) |
| $\lambda$(Mo K$\alpha$) (Å) | 0.71073 | 0.71073 | 0.71073 | 0.71073 |
| crystal system | monoclinic | monoclinic | cubic | monoclinic |
| space group | $P2_1/n$ | $C2/c$ | $P2_13$ (no. 198) | $P2_1/c$ |
| $a$ (Å) | 19.7920(14) | 23.442(2) | 21.248(3) | 20.041(2) |
| $b$ (Å) | 7.9787(6) | 17.302(2) | 21.248(3) | 16.705(2) |
| $c$ (Å) | 21.415(2) | 17.263(2) | 21.248(3) | 23.336(2) |
| $\beta$ (deg) | 113.10(2) | 104.57(1) | 90 | 113.22(3) |
| $V$ (Å$^3$) | 3110.6(4) | 6776.6(13) | 9593(2) | 7179.7(13) |
| $Z$ | 4 | 4 | 4 | 4 |
| $\rho_{calcd}$ (g cm$^{-3}$) | 1.543 | 1.564 | 1.432 | 1.519 |
| $\mu$ (mm$^{-1}$) | 0.851 | 0.887 | 0.907 | 0.680 |
| no of independent reflns ($I > 2\sigma(I)$) | 9037 | 6619 | 5434 | 8681 |
| abs correction | DelRefAbs<br>Platon 1999 | Mulscan Abs<br>Platon 1999 | DelRefAbs<br>Platon 1999 | |
| data/restraints/params | 9000/1/432 | 6562/0/477 | 5411/18/432 | 8581/4/944 |
| $R_F$[a] | 0.0444 | 0.0630 | 0.0697 | 0.0734 |
| abs structure param | | | 0.01(3) | |

[a] $R_F = \sum(|F_o| - |F_c|/\sum|F_c|$.

times with water, and dried over $CaCl_2$ in a vacuum desiccator. Yield: 29.5 g (90%). $^1$H NMR ($CDCl_3$, 250 MHz): $\delta$ 4.60 (s, 2H, $CH_2$), 7.40−7.70 (m, 5H, Ar), ∼9.0 (broad, 1H, NOH). IR (KBr, cm$^{-1}$): 3449 s (br), 1635 m (br), 1071 m, 959 s, 914 s, 770 s, 692 s, 649 s. EI-MS: $m/z$ 169 [$M^+$], 77 ($C_6H_5^+$, 100%).

**1,4,7-Tris(acetophenoneoxime)-1,4,7-triazacyclononanetrihydrochloride, $LH_3 \cdot 3HCl$.** To an ice-cold solution of 1,4,7-triazacyclononane (6.5 g; 50 mmol) in distilled ethanol (50 mL) was added with stirring $\omega$-chloroacetophenoneoxime (25.5 g; 150 mmol) dissolved in 50 mL of absolute ethanol, whereupon the solution became turbid. After addition of $NaHCO_3$ (12.6 g; 150 mmol) the mixture was stirred under ice-cooling for an hour, and then at room temperature for an additional 2 days. The precipitated white solid was filtered off and washed once with cold ethanol. The white solid was suspended in methanol (100 mL) and stirred at ambient temperature for 20 min and then filtered off. This process of suspension and stirring in methanol was repeated altogether four times. The solid was discarded and the united filtrate (∼400 mL) was evaporated under reduced pressure to yield the pure ligand in its trihydrochloride form. Yield: 21.3 g (∼67%). $^1$H NMR ($CD_3OD$, 400 MHz): $\delta$ 7.51−7.53, 7.36−7.43 (m, 15H, Ar), 3.60−3.64 (m, 6H, $CH_2$ of arm), 2.7 (s, 12H, $CH_2$ of ring). IR (KBr, cm$^{-1}$): 3214 s (br, $\nu_{OH}$), 1631 m ($\nu_{CN}$), 959 s ($\nu_{NO}$). MS-ESI pos. in $CH_3OH$: $m/z$ 529.4 [$LH^+$, 100%].

**Preparation of Complexes: $[LH_2Cu^{II}]ClO_4 \cdot CH_3OH$ (1).** To ice-cooled methanol (50 mL) were added the oxime ligand $LH_3 \cdot 3HCl$ (1.28 g; 2 mmol) and $NaClO_4$ (1.4 g; 11.4 mmol) and the suspension was stirred for 0.5 h. The suspension was filtered and to the filtrate was added $Cu(ClO_4)_2 \cdot 6H_2O$ (0.74 g; 2 mmol) along with 10 drops of triethylamine with stirring. The stirring was continued for 0.5 h, whereupon the solution became turbid. The precipitated white solid was filtered off and discarded. Vapor diffusion of diethyl ether yielded X-ray quality blue crystals. Yield: 1.2 g (85%). Anal. Calcd for $C_{31}H_{39}N_6O_4Cu(ClO_4)$: C, 51.52; H, 5.44; N, 11.63. Found: C, 51.7; H, 5.4; N, 12.0. IR (KBr, cm$^{-1}$): 3450 s ($\nu_{OH}$), 1629 m ($\nu_{CN}$), 1121 (sh, $\nu_{NO}$), 1100 s, 623 m ($ClO_4$). UV−vis in $CH_3CN$ ($\epsilon$, $M^{-1}$ cm$^{-1}$): $\lambda$ 670 nm (912). MS-ESI pos. in $CH_3CN$: $m/z$ 590.3 (100%, $LH_2Cu^+$).

**$[L_2Co^{III}_2Co^{II}](ClO_4)_2 \cdot H_2O$, $Et_2O \cdot Me_2CO$ (2) and $[L_2Co^{III}_3](ClO_4)_3$ (2a).** **2** was prepared by the same protocoll as for **1**, using $Co(ClO_4)_2 \cdot 6H_2O$ (0.72 g; 2 mmol) instead of $Cu(ClO_4)_2 \cdot 6H_2O$. A light orange-brown solid was obtained, which was recrystallized from acetone, and vapor diffusion of diethyl ether afforded a mixture of a deep brown microcrystalline substance **2a** and red-orange crystals of **2** suitable for X-ray analysis. Several attempts to obtain a pure sample of **2** proved unsuccessful. Yield: 1.10 g.

Repeated crystallization of the above solid yielded deep brown microcrystals of $[Co^{III}_3L_2](ClO_4)_3$ (**2a**). Anal. Calcd for $C_{60}H_{66}N_{12}O_6Co_3(ClO_4)_3$: C, 47.27; H, 4.36; N, 11.01; Co, 11.58. Found: C, 49.0; H, 4.8; N, 11.1; Co, 11.3. IR (KBr, cm$^{-1}$): 3410 s (br) ($\nu_{OH}$), 1623 m ($\nu_{CN}$), 1147 m (sh) ($\nu_{NO}$), 1100 s, 624 m ($\nu_{ClO_4}$). UV−vis in $CH_3CN$ ($\epsilon$, $M^{-1}$ cm$^{-1}$): $\lambda$ 272 (78670), 448 sh (11700), 655 nm (519). MS-ESI pos. in $CH_3CN$: $m/z$ 585.2 (100%, $CoLH^+$), 1169.2 (20%, $Co_2L_2H_2^+$).

**$[Ni_4(LH)_3](ClO_4)_2 \cdot 3H_2O$ (3).** An ice-cold solution of $LH_3 \cdot 3HCl$ (1.28 g; 2 mmol) in methanol (50 mL) was treated with solid $NaClO_4$ (1.4 g; 11.4 mmol) and the mixture was stirred for 0.5 h, whereupon a white solid separated out. The suspension was filtered to remove the solid and to the clear filtrate was added $Ni(ClO_4)_2 \cdot 6H_2O$ (0.73 g; 2 mmol). The pale yellow-green solution was heated to reflux for 0.5 h and filtered to remove any solid particles. Refrigeration of the filtrate yielded yellow-brown crystals of **3**. Single crystals suitable for X-ray diffraction analysis were grown by diethyl ether vapor diffusion in methanol solution of the complex. Yield: 0.95 (69%). Anal. Calcd for $C_{30}H_{108}N_{18}O_{12}Ni_4(ClO_4)_2$: C, 52.28; H, 5.27; N, 12.19; Ni, 11.35. Found: C, 51.8; H, 5.2; N, 12.3; Ni, 11.5. IR (KBr, cm$^{-1}$): 3420 m ($\nu_{OH}$), 1624 m ($\nu_{CN}$), 1144 m ($\nu_{NO}$), 1100 s, 624 m ($\nu_{ClO_4}$). UV−vis in $CH_3CN$ ($\epsilon$, $M^{-1}$ cm$^{-1}$): $\lambda$ 275 (83400), 286 (sh), 392 (20000), 847 nm (143). MS-ESI pos. in $CH_3CN$: 293 ($NiLH_4^{2+}$), 585.2 (100%, $NiH_2L^+$), 907.2 (5%, $Ni_4L_3H_3^{2+}$), 1169.8 (60%, $Ni_2H_3L^{2+}$), 1227 ($Ni_3L_2H_2$).

**$[L_2Mn^{II}_2(\mu\text{-}O_2COMe)(MeOH)Mn^{III}](ClO_4)_2 \cdot 2MeOH \cdot 3H_2O$ (4).** A methanol solution (50 mL) of $LH_3 \cdot 3HCl$ (0.96 g; 1.5 mmol) and $NaClO_4$ (1.4 g; 8.4 mmol) was stirred for 30 min at 20 °C, after which time the resulting suspension was filtered off. The filtrate was charged with $Mn(ClO_4)_2 \cdot 6H_2O$ (0.65 g; 1.8 mmol), followed by addition of triethylamine (0.4 g; 4 mmol). The reaction mixture was refluxed for 30 min with stirring, after which some brown material was filtered off. Vapor diffusion of ether into the filtrate afforded deep red-brown microcrystals of **4**. Yield: 0.95 g (60%). Anal. Calcd for $C_{65}H_{89}Mn_3N_{12}O_{15}(ClO_4)_2$: C, 47.54; H, 5.46; N, 10.23; Mn, 10.04. Found: C, 47.9; H, 5.4; N, 10.1; Mn, 10.6. IR

(KBr, $cm^{-1}$): 3443 m ($\nu_{OH}$), 1637 s, 1335 m ($\nu_{COO}$), 1140 m (sh) ($\nu_{NO}$), 1110 s, 625 m ($\nu_{ClO_4}$). UV−vis in $CH_3CN$ ($\epsilon$, $M^{-1}$ $cm^{-1}$): $\lambda$ 500 sh nm (1814). MS-ESI pos. in $CH_3CN$: *m*/*z* 608.3 (100%, $[(LH)_2Mn_3]^{2+}$), 1315.5 ($[(LH)_2Mn_3ClO_4]^{+}$).

**CAUTION:** Although we experienced no difficulties with the compounds isolated as their perchlorate salts, the unpredictable behavior of perchlorate salts necessitates extreme caution in their handling.

**Acknowledgment.** This work was partly supported by the Fonds der Chemischen Industrie.

**Supporting Information Available:** X-ray crystallographic files in CIF format. This material is available free of charge via the Internet at http://pubs.acs.org.

IC011322M